



Numerical simulation-based loaded inflation height modeling of nursing bed airbag

Yunxuan Xiao¹ · Teng Liu¹ · Zhong Zhang¹ · Jianjun Zhang¹ · Shijie Guo¹

Received: 7 January 2022 / Accepted: 17 September 2022 / Published online: 24 September 2022
© International Federation for Medical and Biological Engineering 2022

Abstract

In previous studies, the numerical simulation models of industrial airbags were verified to have high accuracy regarding their actual dynamics. However, numerical methods were scarcely utilized to simulate and investigate the inflation height behaviors of nursing bed airbag. For this problem, this study constructs a numerical simulation model illustrating the association between the internal pressure and inflating height of nursing bed airbag, under various external loads. Firstly, based on an averaged pressure prerequisite, an airbag dynamic model is established by the control volume approach (the air inside the airbag follows the gas state equation of Poisson's law). Besides, the elastic mechanical behaviors of airbag film material are determined according to a material constitutive model built by the quasi-static uniaxial tensile test. The obtained data are used as the boundary conditions, for the numerical dynamics modeling of the nursing bed airbag. Verification experiments clarify that this numerical modeling is accurate for describing airbag inflation behaviors, and then can be effectively applied to the design and optimization phases of nursing bed airbags. Based on the simulation modeling above, the mathematical equation of controlling airbag inflating height by its internal pressure is obtained. It provides a vital basis for the differentiated and intelligent control of the airbag nursing bed.

Keywords Airbag nursing bed · Numerical modeling · Control volume method · Airbag internal pressure · Inflating height

1 Introduction

Long-term bedridden patients generally experience serious compression of local tissues [1–3], resulting in blood circulation disorders, tissue nutritional deficiencies, and pressure ulcers (PUs). Complications of PUs such as septicemia have even resulted in the death of some patients [4–6].

Traditionally, for intensive care, timed massage and turning over by nurses are common measures to prevent pressure ulcers in patients. But these methods have many disadvantages, such as high work intensity and infection risk. Therefore, it is urgent to develop an intelligent nursing bed apparatus to adjust the sleeping posture of patients

and prevent pressure ulcers, which has become a consensus among researchers [7–10].

The Body Perfect mattress (USA) monitors the user's physiological information in real time, and perceives their positions, body shapes, and action intentions to actively adjust the user posture [11, 12]. The Leios airbag mattress developed by the University of Tokyo and Molten Corp is equipped with an internal tracker [13], which can analyze whether the user has a comfortable sleeping posture from his recorded daily sleeping activities. Then, Leios has simple temperature control and sleeping posture adjustment capacities. Zhang et al. [14] develop an intelligent airbag mattress to detect and adjust the airbag pressure and height. When people lie on the bed, the bed automatically senses the body structure and pressure, and then adjusts the sleeping position, so as to achieve uniform force distribution and comfortable sleeping position [14]. In addition, Shi et al. [15] summarize evidence from Cochrane Reviews that assess the effects of beds, and mattresses on reducing pressure ulcers and increasing pressure ulcer healing. Based on the study above, compared with foam surfaces, alternating pressure air surfaces may reduce pressure ulcer risk and are

✉ Teng Liu
wuqiu-liu@163.com

¹ State Key Laboratory for Reliability and Intelligence of Electrical Equipment, Hebei Key Laboratory of Robot Perception and Human–Robot Interaction, Hebei University of Technology, School of Mechanical Engineering, Tianjin 300130, China

probably more cost-effective in preventing pressure ulcers [15]. However, these mattresses can hardly accurately regulate the inflation pressure and height of airbags or waterbags, which has poor adaptation for various patients. Therefore, the numerical modeling study onto nursing bed airbags to quantitatively analyze its pressure and height is necessary for its precise inflation control, and thus to realize differentiated care solutions for patients.

With the rapid evolution of computer simulation technology, an increasing number of finite element (FE) modeling methods are adopted to effectively analyze nonlinear dynamic behaviors of hyperelastic material. Elsabbagh [16] establishes a nonlinear dynamic finite element model of an axisymmetric inflatable beam, and then compares the calculated results with testing dates of 2 inflatable beams to verify the modeling accuracy. Graczykowski [17] studies the numerical simulation methods on vibration damping behaviors of 4 adaptive inflatable structures. Wong et al. [18] conduct an Abaqus finite element analysis on the static stiffness characteristics of automotive rolling lobe air spring, demonstrating the nonlinear characteristics of rubber airbags. Based on the model, they analyze the influences of cord angle, cord diameter, and initial internal pressure on the spring vertical static stiffness. These numerical modeling methods and contributions mainly focus on the structural and material properties of hyperelastic material, but the influence of air flow rate and temperature onto its dynamics is scarcely investigated.

To analyze the impact of airflow and temperature changes onto hyperelastic material simulation accuracy, Lee et al. [19] establish an air spring model based on thermodynamics theory. By this model, Lee obtains the influence of the heat transfer and effective area change on the static stiffness and hysteresis characteristics of the air spring, during its working process. Besides, an air spring finite element model is constructed by Oman et al. [20, 21], to analyze the relationship and load deflection characteristics between internal pressure, shapes, and airbag expansion outer diameter. Based on the model above, Oman et al. [20, 21] upgrade the method for the estimation of air spring fatigue life and afterwards used together with finite element analysis to predict the fatigue life and, ultimately, the timing and global location of failure. Regarding the nonlinear behavior of hyperelastic materials, although the research works above have made significant progress on the behavior of hyperelastic materials, these models can hardly accurately mirror the inflating and deflating process of the flexible airbag. Thus, the relationship between airbag pressure and its height cannot be reflected by them.

For this problem, this paper studies the numerical simulation modeling of airbag inflation of nursing beds, and then illustrates the relationship between the airbag internal pressure and its inflating height, under various external loads. The overall logical structure of this paper

is revealed in Fig. 1. Section 2 introduces the airbag nursing bed and inflation measuring experiment for a single airbag. Section 3 determines experimentally the constitutive model of membrane material of nursing bed airbag. Section 4 establishes the simulation model of the airbag inflation process based on experimental data. This model is established by the control volume method (the air inside the airbag follows the gas state equation of Poisson's law). And the comparative experiment is conducted to verify the model accuracy and reveal the dynamic association between the airbag internal pressure and its inflating height. Section 5 builds the mathematical model for controlling airbag inflating height by regulating its internal pressure. Eventually, Section 6 gives conclusions of the whole research.

2 Inflation experiment of nursing bed airbag

2.1 Airbag nursing bed

Generally, the structure of an airbag nursing bed includes 3 parts: airbag, bed body, and airways. According to the functional requirements of the flexible nursing mattress for turning over of patients, the airbag is originally designed as a square single-layer structure. However, the airbag with this structure cannot achieve the proper turning angle (with a limited inflation height), so the airbag structure must be designed to be a double-layer chamber that can swing the head, which is illustrated in Fig. 2.

The double-layer oscillating airbag that has a 100 mm length and a 100 mm width is made of thermoplastic polyurethane elastomer (TPU) material. The airbag mechanical properties are listed in Table 1. It can be inflated to a max of 150 mm height by injecting the air. Airbag arrays are arranged on the nursing bed, and the modules and circuits are hidden under the nursing bed. The control system uses the EtherCAT protocol control method. The solenoid valves with bus control and valve terminal assembly are adopted to simplify the complicated wiring and excessive air pipes under the bed.

According to the bed working principle in Fig. 3, the control system performs a critical function in regulating the behaviors of flexible nursing beds as a whole. It can realize differentiated airbag inflations to achieve the sleeping posture adjustment effect. In order to realize the functions of the airbag nursing bed above, this paper carries out the numerical simulation modeling research based on a single airbag. This research illustrates the relationship between the airbag internal pressure and inflation height under various external loads. And the

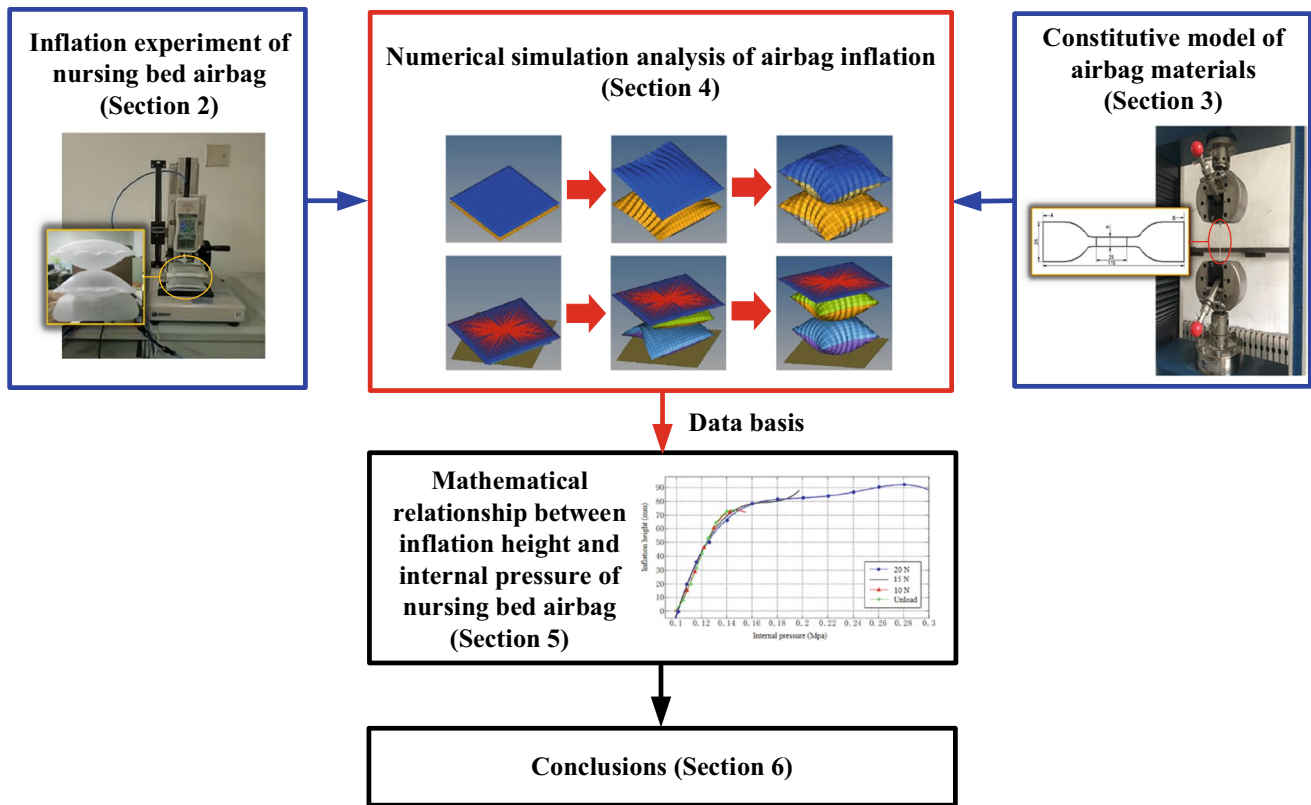


Fig. 1 Logical structure of the paper

airbag inflation measuring experiment is the vital basis for this modeling.

2.2 Inflation measuring experiment for a single airbag

Being the preparation for the finite element simulation modeling of a single airbag, the gas mass flow rate is necessary to be measured during an airbag inflation process. And for the verification of the reliability of this modeling method, the airbag inflation height, airbag internal pressure, and other parameters must be measured during this process as well. The former can be measured by the gas flow meter, and the latter must be realized by a modified material testing machine, which is in Fig. 4. It can monitor the airbag external load by a pressure sensor and ensure it is fixed at a specified value during the airbag inflation process. In this paper, the measured inflation height and internal pressure of the airbag are dynamically displayed in the host computer software, in both the unloaded and loaded airbag states.

It can be seen from Table 2 that both the inflation height and internal pressure of the unloaded airbag increase with time. According to Poiseuille’s law, as the airbag is gradually inflated and deployed, the cross-sectional size of the airbag



Fig. 2 Nursing bed with double-layer airbags

stops increasing, and the pressure difference between the inside and outside of the airbag continues to decrease. Therefore, the gas mass flow rate of the airbag inflation process increases to a peak at 1 s first and then decreases until the inflation ends at 5.5 s, which provides a basis for parameter setting and data comparison of the subsequent airbag inflation simulation.

On the other hand, for the loaded airbag case, the bed plate onto the airbag top must be adopted to facilitate the airbag external vertical loading. Thus, its gravity (0.6 N) must be used to correct the actual external load values in experiments: for example, a 10.4 N external load was

Table 1 Data of the airbag mechanical properties

	Material	Density/kg•mm ⁻³	Poisson's ratio	Length/mm	Width/mm	Thickness/mm
Values	TPU	1.2E-06	0.495	100	100	0.3

Fig. 3 The working principle of airbag nursing bed

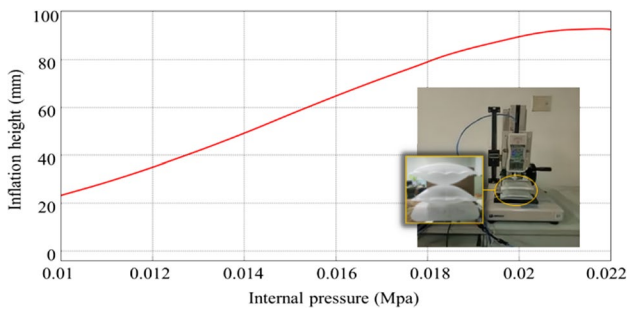
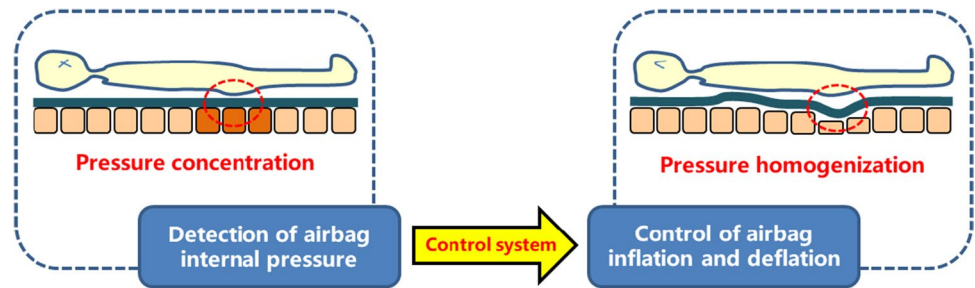


Fig. 4 Relationship curve between airbag inflation height and internal pressure under 1 kg load

applied onto the inflatable airbag, when the load was a weight of 1 kg (9.8 N). During the airbag experiment of this case, the time-varying pressure and height were recorded synchronously, and their correlation curve was clarified in Fig. 4.

As illustrated in this figure, the airbag inflation height grows smoothly with the increase of its internal pressure. Furthermore, a strong correlation between inflation height and its internal pressure is found by the mathematical fitting. The correlation curve above proves that there is a definite mathematical relationship between them, which is discussed in Section 5 (10 N, 15 N, and 20 N external vertical loads are onto the airbag respectively). The correlation curve under various external loads can be revealed in the same way.

Table 2 Unloaded airbag experimental measurements

	1 s	2 s	3 s	4 s	5 s	5.5 s
Airbag heights/mm	20	45	60	65	66	70
Airbag internal pressures/Mpa	8E-03	1E-02	1.200E-02	1.244E-02	1.291E-02	1.297E-02
Air mass flow rates/kg•mm ⁻³	1.935E-07	1.734E-07	1.603E-07	1.005E-07	6.630E-08	6.033E-08

3 Constitutive model of airbag materials

3.1 Energy function of hyperelastic material

The hyperelastic material TPU is used as the airbag film in this paper, and its raw material is mainly oligomer polyol, which is prepared by the (ELS) method [22, 23]. For the incompressible or almost incompressible TPU properties, the tensile test is usually used to determine the model parameters [23–25]. However, under various strains, it is still difficult to determine the constitutive model parameters. Therefore, based on the continuum theory, this paper conducts a finite element modeling on the polyurethane mechanical properties. The common polynomial strain energy function of a hyperelastic material is as follows:

$$W = \sum_{i+j=1}^N C_{ij}(I_1 - 3)^i(I_2 - 3)^j + \sum_{i=1}^N [1/D_i(J - 1)^{2i}] \tag{1}$$

$$I_1 = \lambda_1^2 + \lambda_2^2 + \lambda_3^2 \tag{2}$$

$$I_2 = \lambda_1^2\lambda_2^2 + \lambda_2^2\lambda_3^2 + \lambda_3^2\lambda_1^2 \tag{3}$$

$$I_3 = \lambda_1^2 \lambda_2^2 \lambda_3^2 \tag{4}$$

$$J = I_3^{1/2} \tag{5}$$

where W is the strain energy, N is the function class, I_1, I_2 , and I_3 are defined as the first-order, second-order, and third-order strain invariants, J is the volume ratio, λ_1, λ_2 , and λ_3 are the main extension ratios, C_{ij} is the material constant (Mpa), usually obtained by experimental test, and D_i is the material constant (Mpa^{-1}), which is related to the material compressibility.

The Yeoh model has the advantages of simple form and high accuracy, and its material parameters can be determined based on uniaxial tensile experiments exclusively. When $j=0$ and $N=3$ in Eq. (1), the strain energy density function of the Yeoh model is obtained:

$$W = \sum_{i=1}^3 C_{i0}(I_1 - 3)^i + \sum_{i=0}^3 [1/D_i(J - 1)^{2i}] \tag{6}$$

The material is assumed to be nonstretchable ($I_3 = 1$) and isotropic [26, 27]; meanwhile, the material is always in a uniaxial tensile state during the working process. According to Eq. (5), the simplified function can be obtained:

$$W = \sum_{i=1}^3 C_{i0}(I_1 - 3)^i \tag{7}$$

TPU material being assumed to be incompressible, the relationship between the strain potential energy and the engineering stress can be obtained experimentally in the uniaxial stretching process:

$$\sigma_i = \frac{\partial U}{\partial \lambda_v} = \frac{\partial U}{\partial I_1} \frac{\partial I_1}{\partial \lambda_v} + \frac{\partial U}{\partial I_2} \frac{\partial I_2}{\partial \lambda_v} \tag{8}$$

where σ_i is the engineering stress (Mpa); λ_v is the uniaxial stretching ratio measured by the experimental method. Strain invariants can be obtained:

$$I_1 = \lambda_v^2 + 2\lambda_v^{-1} \tag{9}$$

$$I_2 = \lambda_v^{-2} + 2\lambda_v \tag{10}$$

3.2 TPU membrane quasi-static uniaxial tensile test

The 8 same dumbbell-shaped specimens made of TPU are utilized for the tensile test. The average value of their testing results is obtained to reduce the experimental errors. Thus, the physical properties of the airbag film (TPU) can be obtained based on the quasi-static uniaxial tensile experiment above.

The electronic universal material testing machine developed by Instron Corporation is used to carry out the

uniaxial tensile test of the airbag material. In the experiment, each one of these 8 specimens was mounted respectively to the fixture of the testing machine, and then, the specimen was stretched according to the test standard (Fig. 5).

In order to eliminate the viscoelasticity effect, the tensile test is needed to be carried out at a low rate: the lower clamp is kept to be stationary, and the upper clamp is used to pull the specimen vertically upward at a 100 mm/min stretching rate, to obtain the specimen stress–strain curve. Moreover, for eliminating the experimental error, 8 specimens were subjected to the tensile test under the same conditions, to obtain an averaged stress–strain curve. Finally, the Yeoh model in Abaqus is used for finite element simulation of the dumbbell-shaped specimen. The simulation result with the Yeoh model is compared and agreed with the corresponding experimental data, which is shown in Fig. 6.

4 Numerical simulation analysis of airbag inflation

4.1 Governing equations of airbag inflation simulation

The control volume method based on the uniform pressure prerequisite is a common method for airbag inflation simulation. For the transient simulation, the airbag inflation is regarded as an adiabatic process; moreover, the airbag internal temperature and pressure remain uniform at any moment. The values of mass flow rate and temperature are set in simulation for describing the injected gas. Since the inflation direction and surface area of the airbag at each time step are known, its real-time volume can be obtained by Green’s integral theorem:

$$V = \iiint dx dy dz = \oint x n_x d\Gamma \approx \sum_{i=1}^N \bar{x}_i n_{ix} A_i \tag{11}$$

where \bar{x}_i is the mean value of the element coordinates, n_{ix} is the angle cosine between the element normal direction and the X direction, and A_i is the unit area. With the airbag gas being assumed to be an ideal gas (its heat capacity remains constant), its specific thermodynamic energy can be determined by the airbag volume at any time:

$$e_2 = e_1 \left(\frac{V_1}{V_2} \right)^\gamma \tag{12}$$

where V is the airbag volume, γ is the gas-specific heat ratio, $\gamma = C_p/C_v$, C_p is the heat capacity at the constant pressure ($\text{J}\cdot\text{kg}^{-1}\text{K}^{-1}$), C_v is the heat capacity at the constant volume ($\text{J}\cdot\text{kg}^{-1}\text{K}^{-1}$), e is the specific thermodynamic energy, $e = E/\rho_0$, E is the thermodynamic energy (J), and ρ is the

Fig. 5 Material tensile test

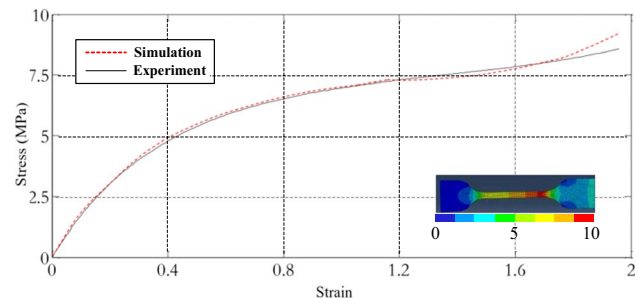
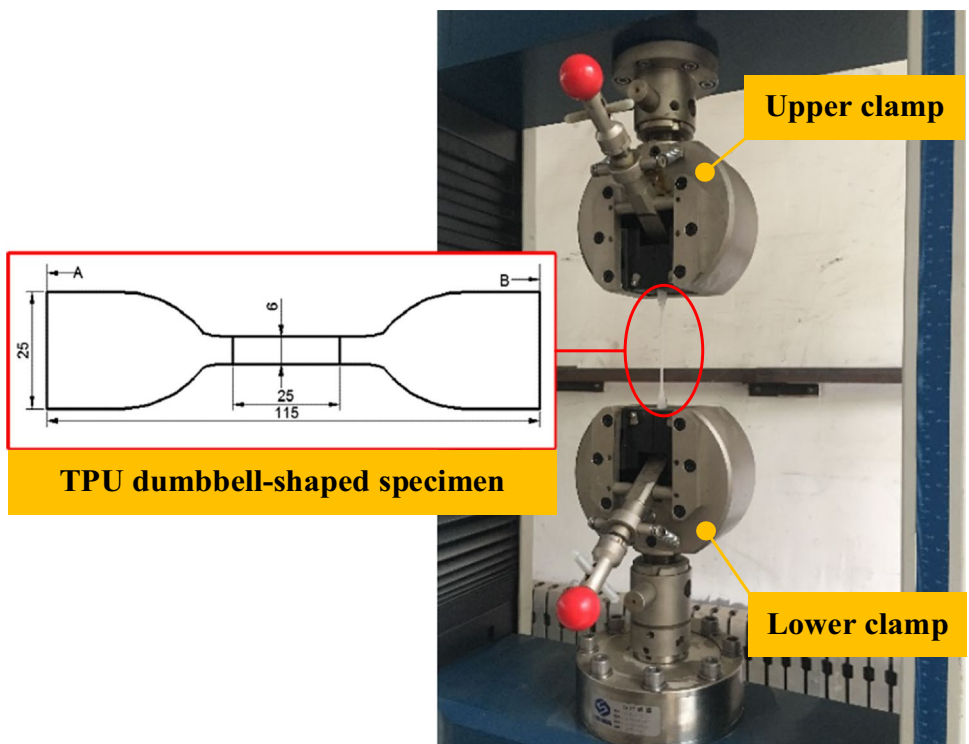


Fig. 6 Comparison of simulation and experimental curves of Yeoh model

density (kg/m). Therefore, e_2 can be calculated, with the given data e_1 , V_1 and V_2 . Furthermore, the airbag internal pressure can be computed by the gas equation of state:

$$pV^\gamma = p_1V_1^\gamma = p_2V_2^\gamma = C \tag{13}$$

$$E = \frac{m}{M} C_{v,m} T \tag{14}$$

$$E = \int_{V_1}^{V_2} p dV \tag{15}$$

$$p = (\gamma - 1)\rho e \tag{16}$$

where p is the pressure (MPa), C is the constant, m is the gas quality (kg), M is the gas molar mass, $C_{v,m}$ is the molar heat capacity at the constant volume ($\text{J}\cdot\text{mol}^{-1}\text{K}^{-1}$), and T is the temperature (K). The gas quality in the airbag has the following relationship:

$$\dot{m} = \dot{m}_{in} + \dot{m}_{out} \tag{17}$$

where \dot{m} is the gas mass flow rate (kg/ms), \dot{m}_{in} is the gas mass flow rate inflated into the airbag, $\dot{m}_{out} = \dot{m}_{vent} + \dot{m}_{leak}$, \dot{m}_{vent} is the gas mass flow rate through the vent, and \dot{m}_{leak} is the mass flow rate leaked from the airbag surface. The airbag gas pressure under adiabatic conditions meets the following relationship:

$$\frac{p}{\rho^\gamma} = \frac{p_{out}}{\rho_{out}^\gamma} = C \tag{18}$$

where p_{out} is the vent gas pressure; ρ_{out} is the vent gas density. The Bernoulli equation for compressible fluids can be expressed as:

$$g dz + \frac{dp}{\rho} + \frac{1}{2} d(v^2) = 0 \tag{19}$$

where v is the flow velocity (mm/ms), g is gravitational acceleration, z is the height (mm), and the potential energy term ($g dz$) is ignored due to its little changes. According to Eq. (16), the simplified function can be obtained:

$$\frac{\gamma}{\gamma - 1} \frac{p}{\rho} = \frac{\gamma}{\gamma - 1} \frac{p_{out}}{\rho_{out}} + \frac{u^2}{2} \tag{20}$$

where u is the gas flow rate in the vent (mm/ms), and u can be calculated:

$$u^2 = \frac{2\gamma}{\gamma - 1} \frac{p}{\rho} \left(1 - \left(\frac{p_{out}}{p} \right)^{\frac{\gamma-1}{\gamma}} \right) \tag{21}$$

the mass flow rate and the thermodynamic energy flow rate can be calculated:

$$\dot{m}_{out} = \rho_{out} u A \rho \left(\frac{p_{out}}{p} \right)^{\frac{1}{\gamma}} u A \tag{22}$$

$$\dot{E}_{out} = \dot{m}_{out} \frac{E}{\rho V} = \left(\frac{p_{out}}{p} \right)^{\frac{1}{\gamma}} u A \frac{E}{V} \tag{23}$$

where A is the cross-sectional area of the vent (mm²).

4.2 Finite element simulation modeling of airbag inflation process

4.2.1 Airbag simulation modeling method under various load conditions

As described in Section 2.2, necessary parameters are measured during the airbag inflation experiments, for its finite element numerical simulation modeling. On one hand, the gas mass flow rate during the airbag inflation process is measured to be used as the simulation boundary conditions. On the other hand, some parameters such as the airbag inflation height and internal pressure are monitored during the airbag inflation process, to verify the reliability of the numerical simulation modeling method of the airbag inflation process.

Based on these detections, airbag inflation experiments are performed with specified external vertical loads 0 N (unloaded state), and 10 N, 15 N, and 20 N. Empirically, a common human body has a 10~25 N force range of the pressure concentration position when this person is lying down [28]. Therefore, states 10 N, 15 N, and 20 N of the loaded airbag are reasonable according to the actual application of the airbag nursing mattress.

Correspondingly, the airbag numerical simulation model is established according to these unloaded and loaded airbag states above: As revealed in Fig. 7, the elastic double-layer airbag with a middle connection is meshed by linear square membrane elements. For the meshed model, the airbag outer surfaces are considered to be a closed surface except for the vent hole, and the air at room temperature is set as the inflated gas. Besides, for the finite element simulation, the bed plate and the load imposed by the person are considered

to be rigid. Thus, a rigid body model is established onto the airbag top, to realize the vertical loading onto it. It is meshed by shell elements, and lifted vertically as the airbag is injected with air from its bottom inlet. The detected mass flow curve mentioned above is defined as the input curve of the airbag inflation. In addition, the relevant material parameters of this airbag model are in Table 1.

4.2.2 Comparison and discussion about airbag inflation simulation results

For the simulation, the airbag is inflated by injecting the air at the rate adopted by the previous airbag inflation experiment. Figure 8 reveals the simulation results of the airbag inflation process, and Fig. 9(a) demonstrates the comparison curves of inflation height and internal pressure of the unloaded model. The comparison curve proves the reliability of the simulation model from the aspects of the change trend and numerical value, which has reference value for similar elastomer modeling activities.

It can be seen from the comparisons that the simulation results of the unloaded airbag inflation height are consistent with their experimental results. Thus, the modeling method is reliable to describe the airbag inflation behaviors. Besides, in Fig. 9(a), different from the increasing trend of airbag height in its inflation experiment, the simulation curve of airbag inflation height fluctuates slightly at the end of the inflation stage. The slight error in the simulation curve is due to the measurement error of the mass flow curve obtained experimentally, which causes the gas filling speed to be less than its leakage speed from the airbag at the end of the inflation process. Figure 9(b) clarifies that the maximum internal pressure during the whole inflation process is approximately equal to the pressure of pressure-reducing valve. Unlike the experimental curve, the simulation curve shows that the pressure suddenly drops when the inflation pressure reached its peak, and then gradually rises again. The reason for this phenomenon is found in the comparison with an experiment: when the airbag is close to full state, the airbag edge shape changed from convex to concave, which leads to the

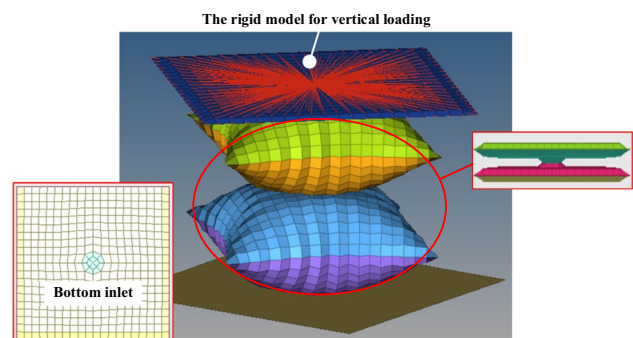


Fig. 7 Airbag finite element model with vertical loading

sudden volume growth of the airbag and its internal pressure drops, but the actual internal pressure curve is not accurate due to the sensitivity of the experiment equipment. However, it is worth affirming that the simulation situation is consistent with the actual inflation process, which also proves the correctness of the airbag inflation simulation model.

Based on the airbag inflation experiment, for the airbag to be inflated to a predetermined height under a certain load, the air mass flow of the airbag (the maximum pressure of the pressure-reducing valve) needs to be continuously adjusted. At this time, the airbag inflation experiment data should correspond to the simulation input data. The simulation results of the airbag inflation process with a 10 N load are described in Fig. 10, and the

simulation results are consistent with the actual airbag inflation process. During this process, the airbag edge is folded inward slightly, but as the gas mass increased, the airbag volume gradually grows to a full state. In addition, the inflation simulation processes under other load conditions are consistent with the case above.

The airbag internal pressure and inflation height comparison curves of 3 different external loads are shown in Fig. 11. For the actual airbag measurement experiment with various loads, as the load increases, the preset pressure of the pressure-reducing valve required for the airbag inflation also increases, and the preset pressure is also the airbag maximum internal pressure when it inflates to its highest height. For the airbag full state,

Fig. 8 Finite element model of unloaded airbag inflation process

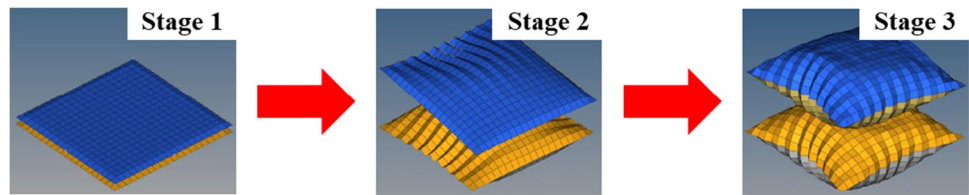
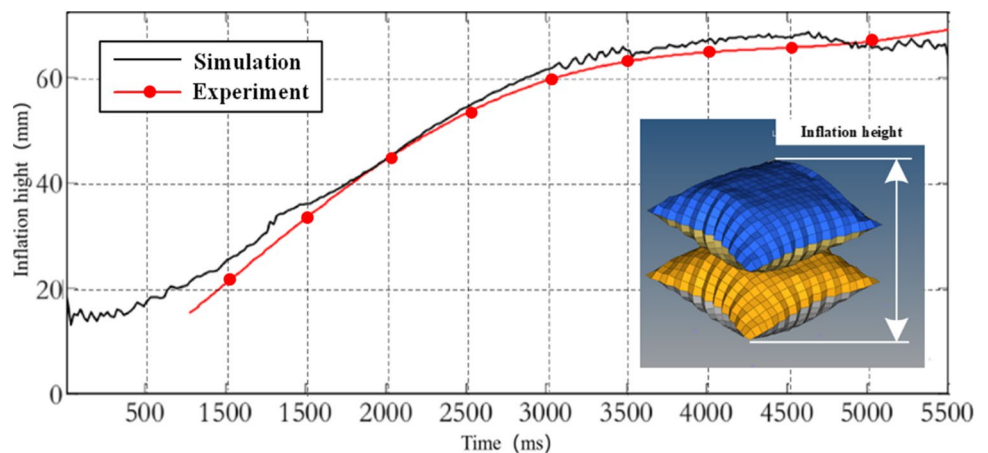
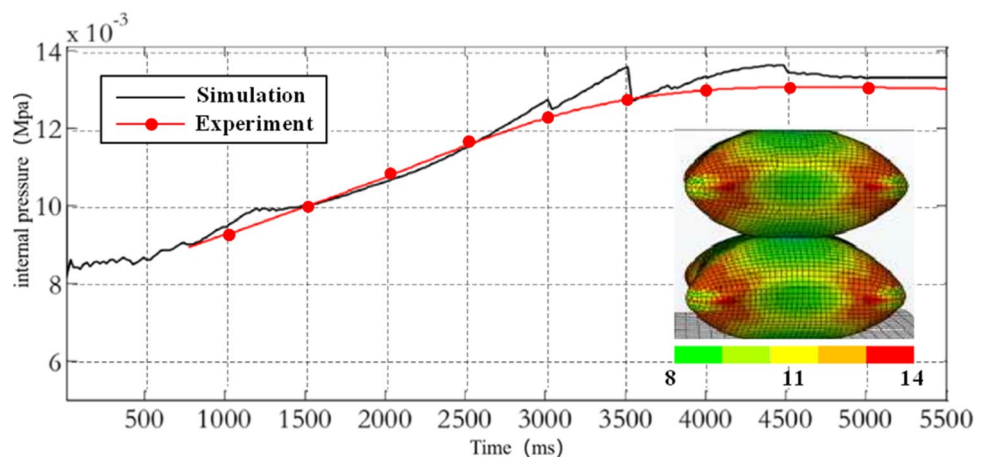


Fig. 9 Comparisons of simulated curve and their corresponding experimental data

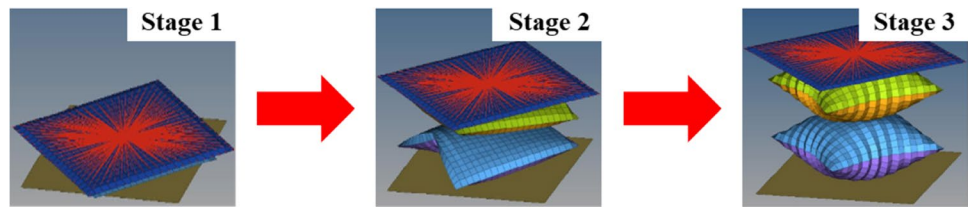


(a) the comparison curve of the inflation height of the unloaded model



(b) the comparison curve of the internal pressure of the unloaded model

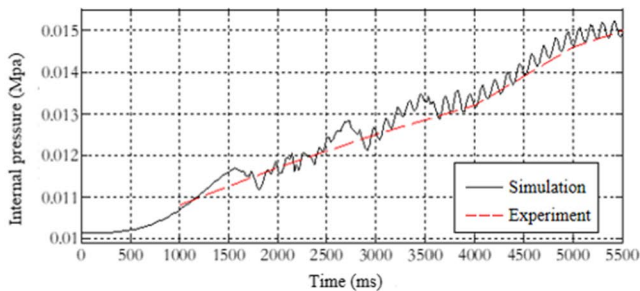
Fig. 10 Finite element model of 10 N loaded airbag inflation process



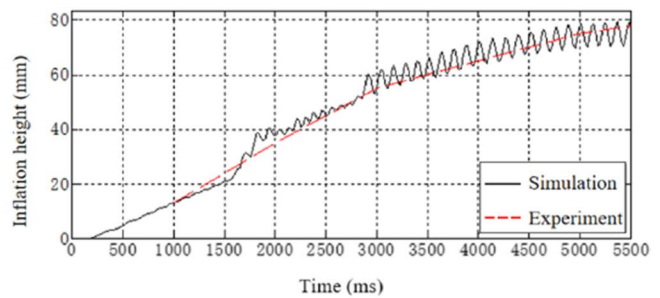
the volume and inflation height of the airbag are directly proportional to the gas pressure caused by the pressure-reducing valve, so the maximum value of the airbag inflation height and its internal pressure will increase with the increase of the load. Besides, it can be seen that the simulation curve has slight fluctuations due to the airflow variations, but the entire inflation process has the agreement with the actual experiment, which proves the reliability of the simulation model. This simulation modeling method can be effectively used into the design and optimization phases of nursing bed airbags.

5 Mathematical relationship between the inflation height and internal pressure of nursing bed airbag

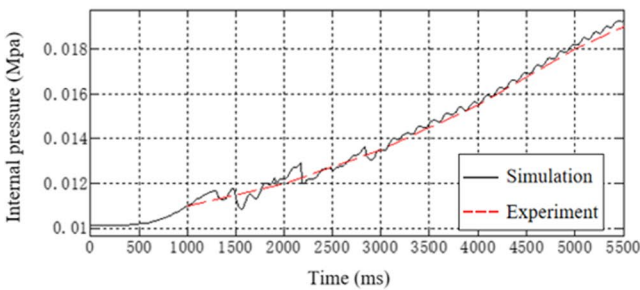
For the established simulation models of airbag inflations with various external loads, the relationship between the airbag inflation height and its internal pressure can be investigated respectively. After fitting the data by polynomial, the correlation curves of airbag inflation height with its internal pressure under various loads are obtained, which is shown in Fig. 12.



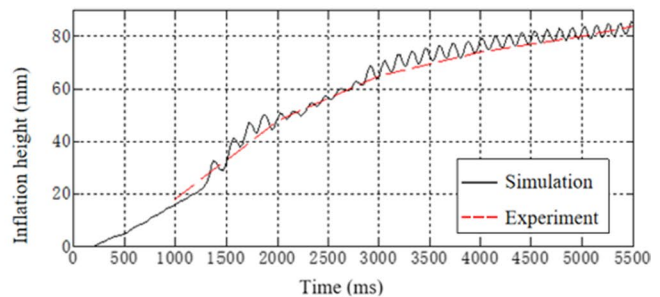
(a) Internal pressure, 10N



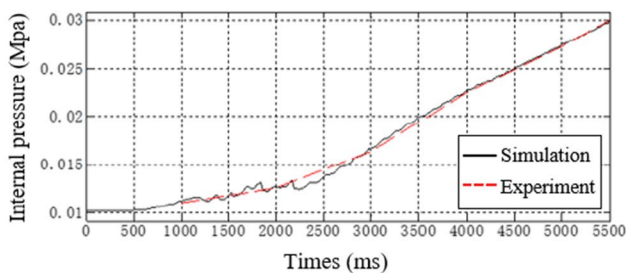
(b) Inflation height, 10N



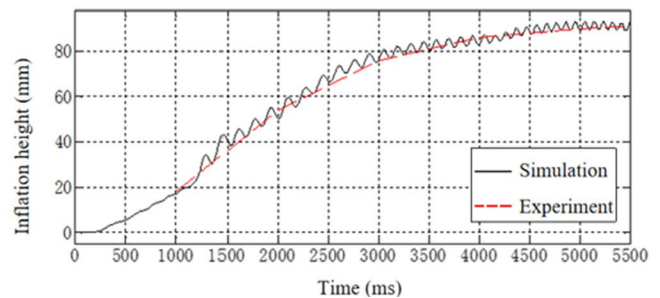
(c) Internal pressure, 15N



(d) Inflation height, 15N



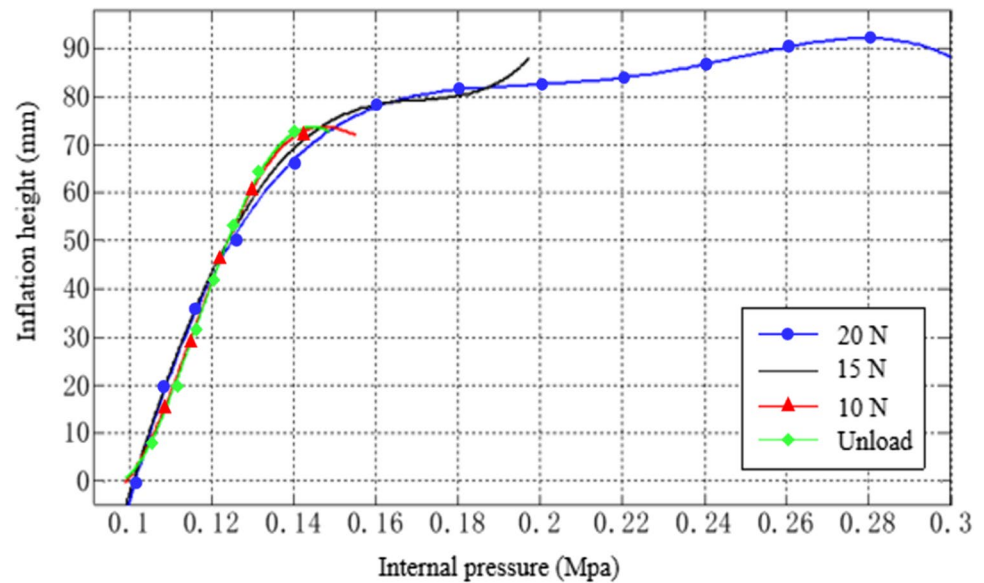
(e) Internal pressure, 20N



(f) Inflation height, 20N

Fig. 11 Comparisons of simulated curves and their corresponding experimental data under various airbag vertical loads

Fig. 12 Correlation curve between airbag inflation height and internal pressure



For the reasons described above, the maximum airbag inflation height and its internal pressure increase with the increasing load, and there is a strong correlation between the maximum inflation height and its internal pressure. Therefore, although there are various values of input conditions (such as gas mass flow rate and external load) for airbag inflation simulations, these simulations obtain correlation curves with similar shapes and trends.

Simultaneously, the simulation results show that under the same conditions, for a given airbag, there is a definite correspondence between the airbag internal pressure scale and its inflation height. This numerical relationship does not vary with the variations of gas mass flow rate and the airbag external load. Therefore, it is of great significance to find the relationship between the airbag internal pressure and inflation height, and then explore the dynamic characteristic curve of a given airbag to achieve accurate posture adjustment of airbag nursing beds under various human body loads.

The correlation curve is polynomial-fitted based on MATLAB, and the following parameter formulas are obtained (the confidence interval is 95%):

$$h = p_1 * x^4 + p_2 * x^3 + p_3 * x^2 + p_4 * x + p_5 \quad (24)$$

$$p_1 = -4.603e + 05(-4.759e + 05, -4.447e + 05) \quad (25)$$

$$p_2 = 4.099e + 05(3.978e + 05, 4.220e + 05) \quad (26)$$

$$p_3 = -1.349e + 05(-1.383e + 05, -1.315e + 05) \quad (27)$$

$$p_4 = 1.955e + 04(1.914e + 04, 1.996e + 04) \quad (28)$$

$$p_5 = -9.741e + 02(-9.917e + 02, -9.564e + 02) \quad (29)$$

where x is the airbag internal pressure (MPa), h is the airbag inflation height (mm), and p is the fitting parameter.

According to the relationship above, the airbag internal pressure is adjusted by controlling the total mass of air filled into the airbag, and then the airbag is inflated to a specific height to achieve effective posture adjustment, which greatly simplifies the control of the multifunctional flexible airbag nursing bed.

6 Conclusion

In order to realize the precise and flexible control of the array airbag nursing bed, this paper conducts research on the numerical modeling method of loaded airbag inflation of nursing beds. Firstly, the hyperelastic materials constitutive model is established based on the uniaxial tensile experiment of airbag film materials, which provides material property parameters for the airbag inflation process modeling. Subsequently, the airbag inflation process is simulated, and then, the mathematical relationship between airbag inflation height and its internal pressure changes is proposed in this paper. The conclusions of this study are as follows:

1. The quantitative inflation process of the nursing bed airbag can be described by the numerical simulation modeling method adopted in this paper. Its accuracy is verified by the agreement between simulation results and experimental data. The presented numerical modeling method can be utilized into the design and optimization of nursing bed airbags.
2. Based on experiments and simulations, the mathematical relationship between the inflation height and internal pres-

sure of nursing bed airbags is illustrated. This relationship can be adopted for the accurate control of a flexible nursing bed airbag, and then provides a basis for a differentiated and intelligent control strategy of the nursing bed with array airbags, for patients to turn over and prevent pressure ulcers.

Study prospect: in this paper, the relevant experiments and simulation analysis are mainly carried out based on a single airbag, without coupling the human body model as a whole with the array airbag model. On the other hand, for the preparation of the intelligent control strategy study of the nursing bed with array airbags, the mathematical model of array airbag inflations influenced by differentiated airbag internal pressures must be established. But this work is not covered in this paper.

In order to overcome these weaknesses and limitations, our future work will be the whole human body–array airbag inflations coupling modeling method, which is influenced by differentiated airbag internal pressures. It must be based on the proposed mathematical relationship between airbag inflation height and its internal pressure changes in this paper. Then, the intelligent control strategy of the nursing bed with an array of airbags will also be studied, for patients to turn over and prevent pressure ulcers.

Author contribution Yunxuan Xiao implemented the whole study and wrote the initial draft of the manuscript. Teng Liu designed the study and gave Yunxuan Xiao significant guidance about the numerical simulation modeling method of loaded airbag inflation. Zhong Zhang participated in experiment preparation and data collection. Jianjun Zhang gave crucial comments onto this work for improving its technical route. Shijie Guo contributed to analyses and interpretations of data and assisted in the model verification.

In short, all authors contributed to the study conception and design. All authors approved the final manuscript and were accountable for the study, ensuring that data generated or analyzed in this study are available.

Funding The authors received the fund of the National Key R&D Program of China (No. 2021YFC0122700) and the fund of the National Nature Science Foundation of China (No.61871173).

Declarations

Ethical approval Not applicable.

Consent to participate All authors consent to participate in the author team of this submitted manuscript.

Consent for publication The submitted manuscript is approved by all its authors for publication.

Competing interests The authors declare no competing interests.

References

- Cortés OL, HerreraGalindo M, Villar JC, Rojas YA et al (2021) Frequency of repositioning for preventing pressure ulcers in patients hospitalized in ICU: protocol of a cluster randomized controlled trial. *BMC Nurs* 20(1):121–121. <https://doi.org/10.1186/S12912-021-00616-0>
- Serrano Lima M, González Méndez MI, Carrasco Cebollero FM, Lima Rodríguez JS (2017) Risk factors for pressure ulcer development in Intensive Care Units: a systematic review. *Med Intensiva (English Edition)* 41(6):339–346. <https://doi.org/10.1016/j.medine.2017.04.006>
- Rabadi MH (2021) Fever in a paraplegia patient with a pressure ulcer. *Radiol Case Rep* 16(9):2434–2436. <https://doi.org/10.1016/j.radcr.2021.05.065>
- Lindqvist EK, Sommar P, Stenius M, Lagergren JF (2020) Complications after pressure ulcer surgery - a study of 118 operations in spinal cord injured patients. *J Plast Surg Hand Surg* 54(3):145–150. <https://doi.org/10.1080/2000656X.2020.1720700>
- Anoop RG, Kareem JK, Murillo A, Taylor DO et al (2019) Post-operative pressure ulcers after geriatric hip fracture surgery are predicted by defined preoperative comorbidities and postoperative complications. *J Am Acad Orthop Surg* 28(8):1–1. <https://doi.org/10.5435/JAAOS-D-19-00104>
- Chopra T, Kaye K, Sobel J (2017) Gunshot injury paraplegics—a population dying a slow, irreversible, and expensive death—a viewpoint on preventing pressure ulcers. *Infect Control Hosp Epidemiol* 38(6):759–760. <https://doi.org/10.1017/ice.2017.33>
- Shi C, Dumville JC, Cullum N, Rhodes S et al (2021) Beds, overlays, and mattresses for treating pressure ulcers. *Cochrane Database Syst Rev* 5:CD013624–CD013624. <https://doi.org/10.1002/14651858.cd013624>
- Prado C, Machado E, Mendes K, Silveira R et al (2021) Support surfaces for intraoperative pressure injury prevention: systematic review with meta-analysis. *Rev Lat Am Enfermagem* 29(8):e3493. <https://doi.org/10.1590/1518-8345.5279.3493>
- De Oliveira K F, Nascimento K G, Nicolussi A C, Chavaglia S R R, et al. (2017) Support surfaces in the prevention of pressure ulcers in surgical patients: an integrative review. *Int J Nurs Pract* 23(4). <https://doi.org/10.1111/ijn.12553>.
- Jiang J, Liu T, Zhang Y et al (2017) Design and development of an intelligent nursing bed — a pilot project of “joint assignment”. *IEEE Engineering in Medicine and Biology Society. Annu Conf* 2017:38–41. <https://doi.org/10.1109/EMBC.2017.8036757>
- Gherzi I, Mari OM, Miralles MT (2016) From modern push-button hospital-beds to 20th century mechatronic beds: a review. *J Phys: Conf Ser* 705(1):012054. <https://doi.org/10.1088/1742-6596/705/1/012054>
- Gherzi I, Mariño M, Miralles MT (2018) Smart medical beds in patient-care environments of the twenty-first century: a state-of-art survey. *BMC Med Informat Decis Making* 63(18). <https://doi.org/10.1186/s12911-018-0643-5>.
- Vest JR, Jung HY, Wiley JR et al (2019) Adoption of health information technology among US nursing facilities. *J Am Med Dir Assoc* 20(8):995–1000. <https://doi.org/10.1016/j.jamda.2018.11.002>
- Zhang Z, Jin X, Wan Z, et al (2021) A feasibility study on smart mattresses to improve sleep quality. *J Healthcare Eng* 6127894. <https://doi.org/10.1155/2021/6127894>
- Shi C, Dumville JC, Cullum N et al (2021) Beds, overlays and mattresses for preventing and treating pressure ulcers: an overview of Cochrane Reviews and network meta-analysis. *Cochrane Database Syst Rev* 8(8):CD013761. <https://doi.org/10.1002/14651858.CD013761.pub2>
- Elsabbagh A (2015) Nonlinear finite element model for the analysis of axisymmetric inflatablebeams. *Thin-Walled Struct* 96:307–313. <https://doi.org/10.1016/j.tws.2015.08.021>
- Graczykowski C (2016) Mathematical models and numerical methods for the simulation of adaptive inflatable structures for impact absorption. *Comput Struct* 174:3–2. <https://doi.org/10.1016/j.compstruc.2015.06.017>

18. Wong PK, Xie Z, Zhao J et al (2014) Analysis of automotive rolling lobe air spring under alternative factors with finite element model. *J Mech Sci Technol* 28(12):5069–5081. <https://doi.org/10.1007/s12206-014-1128-9>
19. Lee SJ (2010) Development and analysis of an air spring model. *Int J Automot Technol* 11(4):471–479. <https://doi.org/10.1007/s12239-010-0058-5>
20. Oman S, Nagode M (2013) On the influence of the cord angle on air-spring fatigue life. *Eng Fail Anal* 27(1):61–73. <https://doi.org/10.1016/j.engfailanal.2012.09.002>
21. Oman S, Nagode M (2018) The influence of piston shape on air-spring fatigue life. *Fatigue Fract Eng Mater Struct* 41(5):1019–1031. <https://doi.org/10.1111/ffe.12748>
22. Khandan A, Jazayeri H, Fahmy MD et al (2017) Hydrogels: types, structure, properties, and applications. *Front Biomater Bentham Sci* 4(27):143–169
23. Heydary HA, Karamian E, Poorazizi E et al (2015) A novel nanofiber of iranian gum tragacanth-polyvinyl alcohol/nanoclay composite for wound healing applications. *J Mater Process Technol* 11(2015):176–182. <https://doi.org/10.1016/j.mspro.2015.11.079>
24. Pearce S (2012) Effect of strain-energy function and axial pre-stretch on the bulges, necks and kinks forming in elastic membrane tubes. *Math Mech Solids* 17(8):860–875. <https://doi.org/10.1177/1081286511433084>
25. Pawlikowski M (2014) Non-linear approach in visco-hyperelastic constitutive modelling of polyurethane nanocomposite. *Mech Time-Dependent Mater* 18(1):1–20. <https://doi.org/10.1007/s11043-013-9208-2>
26. Ogden R (1972) Large deformation isotropic elasticity-on the correlation of theory and experiment for incompressible rubberlike solids. *Proceedings of the Royal Society of London. Math Phys Sci* 326(1567):565–584. <https://doi.org/10.1098/rspa.1972.0096>
27. Venter MP, Venter G (2012) Overview of the development of a numerical model for an inflatable paper dunnage bag. *Packag Technol Sci* 25(8):467–483. <https://doi.org/10.1002/pts.991>
28. Winter DA (2009) *Biomechanics and motor control of human movement*, 4th edn. John Wiley & Sons Inc, New York

Publisher's note Springer Nature remains neutral with regard to jurisdictional claims in published maps and institutional affiliations.

Springer Nature or its licensor holds exclusive rights to this article under a publishing agreement with the author(s) or other rightsholder(s); author self-archiving of the accepted manuscript version of this article is solely governed by the terms of such publishing agreement and applicable law.



Yunxuan Xiao received a B.S. degree from Shijiazhuang Tiedao University in 2018. He is currently pursuing a Ph.D. degree at the Hebei University of Technology. His main research interest includes nursing assistant beds.



Teng Liu received his D.E. degree in mechanical engineering from Tianjin University in 2016. He has been an associate professor and supervisor of master students at the School of Mechanical Engineering, Hebei University of Technology, in Tianjin since 2019.



Zhong Zhang received a B.S. degree from the North China Institute of Aerospace Engineering in 2020. He is currently pursuing a master's degree at Hebei University of Technology. His main research interest includes nursing assistant beds.



Jianjun Zhang received his D.E. degree in mechanical engineering from Beihang University in 2004. He has been a professor (since 2009) and supervisor of doctor students (since 2015) at the School of Mechanical Engineering, Hebei University of Technology, in Tianjin. His main research interest includes the mechanism and intelligent rehabilitation robots.



Shijie Guo received his D.E. degree in mechanical engineering from the Tokyo Institute of Technology in 1992. He has been a professor (since 2015) and supervisor of doctor students (since 2015) at the School of Mechanical Engineering, Hebei University of Technology, in Tianjin. He also serves as a professor of the Institute of AI and Robotics at Fudan University, and the principal scientist of the State Key Laboratory for Reliability and Intelligence of Electrical Equipment. His current research interests are nursing systems including transfer assistant robots, intelligent nursing beds, and unconstrained measurement of vital information.